A&A 466, 501–507 (2007)
DOI: 10.1051/0004-6361:20054536

Astronomy & Astrophysics

Carbon stars and C/M ratio in the WLM dwarf irregular galaxy⋆

A. T. Valcheva[1], V. D. Ivanov[2], E. P. Ovcharov[1], and P. L. Nedialkov[1]

[1] Department of Astronomy, University of Sofia, 5 James Bourchier, Sofia 1164, Bulgaria
e-mail: [valcheva;evgeni;japet]@phys.uni-sofia.bg
[2] European Southern Observatory, Ave. Alonso de Cordova 3107, Casilla 19, Santiago 19001, Chile
e-mail: vivanov@eso.org

Received 17 November 2005 / Accepted 18 January 2007

ABSTRACT

We identify the rich carbon star population of the Magellanic-type dwarf irregular galaxy WLM (Wolf-Lundmark-Melotte) and study its photometric properties from deep near-IR observations. The galaxy also exhibits a clear presence of oxygen-rich population. We derive a carbon to M-star ratio of $C/M = 0.56 \pm 0.12$, relatively high in comparison with many galaxies. The spatial distribution of the AGB stars in WLM hints at the presence of two stellar complexes with a size of a few hundred parsecs. Using the H I map of WLM and the derived gas-to-dust ratio for this galaxy $N(\mathrm{H\,I})/E(B-V) = 60 \pm 10$ [10^{21} at. cm^{-2} mag^{-1}] we re-determined the distance modulus of WLM from the IR photometry of four known Cepheids, obtaining $(m-M)_0 = 24.84 \pm 0.14$ mag. In addition, we determine the scale length of 0.75 ± 0.14 kpc of WLM disk in the J-band.

Key words. galaxies: individual: WLM – stars: AGB and post-AGB – stars: carbon – galaxies: irregular – Local Group

1. Introduction

WLM (Wolf-Lundmark-Melotte; also DDO 221; Wolf 1909; Melotte 1926) is a dwarf irregular Local Group member. Earlier photographic surveys of the galaxy were presented in Ables & Ables (1977) and Sandage & Carlson (1985). The first CCD observations of WLM were performed by Ferraro et al. (1989), who reported significant variations in the recent star-formation rate across the galaxy. They also detected a uniform underlying relatively old stellar population (∼1 Gyr). Later on, Minniti & Zijlstra (1997) derived a distance modulus $(m - M)_0 = 24.75 \pm 0.1$ mag and [Fe/H] $= -1.45 \pm 0.2$ from V- and I-band photometry. Hodge et al. (1999) reported the first *HST* observations of WLM. They resolved the sole globular cluster (Ables & Ables 1977) and obtained $(m - M)_0 = 24.73 \pm 0.07$ mag, [Fe/H] $= -1.52 \pm 0.08$, and an age of 14.8 ± 0.6 Gyr, typical for the old globulars in the Milky Way. Dolphin (2000) concluded that the WLM started to form stars about 12 Gyr ago, with approximately half of the star-formation occurring during the last 9 Gyr, also based on *HST* imaging.

Recently, Venn et al. (2003) determined [Fe/H] $= -0.38 \pm 0.29$ from high-resolution spectroscopy of two WLM blue supergiants. They found depleted stellar oxygen abundance by a factor of five, in comparison with the oxygen abundance of the H II regions. Even though later Lee et al. (2005) reduced the discrepancy, some unusual chemical evolution history is required to explain the observations because the enhanced stellar abundance would put WLM well above the metallicity–luminosity relation.

These results make it important to study the carbon stars in WLM because of their sensitivity to the metal abundance. Besides, AGB stars are representative of the stellar population with ages between 1–10 Gyr and can be used as an observational constraint to the properties of the post-main sequence stellar evolution. Initially, the behavior of the C/M ratio is understood at least qualitatively (Scalo & Miller 1981; Iben & Renzini 1983). A large number of studies of AGB stars in Local Group galaxies were performed using optical narrow-band imaging. It turns out to be an easy way to separate M-type from carbon stars (Albert et al. 2000; Battinelli & Demers 2004). The progress in recent years made it possible to produce the first observational calibrations of the C/M ratio versus metallicity relation (Groenewegen 2006; Cioni & Habing 2005; Battinelli & Demers 2005).

As AGB stars are almost the brightest cool stars it is easy to investigate them in the near-IR range. The interest in this region of the spectrum grew strongly in the last three years (Cioni & Habing 2003, 2005; Kang et al. 2005, 2006; Sohn et al. 2006). Here we report on the analysis of the carbon stars in WLM from near-IR imaging.

2. Observations and data reduction

The observations of WLM were made in Dec. 2004 under non-photometric conditions. To estimate the foreground contamination, an additional field located 14.8 arcmin South from the center of the galaxy, far enough to eliminate the galaxy contribution, was observed in July 2006 (hereafter "clear sky" field). The near-IR imaged and spectrograph SofI (Son of ISAAC) at the ESO NTT (New Technology Telescope) on La Silla was used. The instrument is equipped with a 1024 × 1024 Hawaii HgCdTe array with 18.5 micron square pixels and a scale of 0.288 arcsec pixel^{-1}, giving a field of view of 4.92 × 4.92 arcmin^2. We alternated between the target and a clear patch of sky nearby. To minimize the effects of array cosmetics and to improve the sky subtraction, we introduced a small random jitter of up to a few tens of arcseconds between the sequential images. In total, we collected 10 images for both fields in J_S and 20 on the galaxy and 15 on the "clear sky" field in K_S. Each of the images in J_S is the average of 2 × 30 s exposures and of

⋆ Full Table 1 is only available in electronic form at http://www.aanda.org

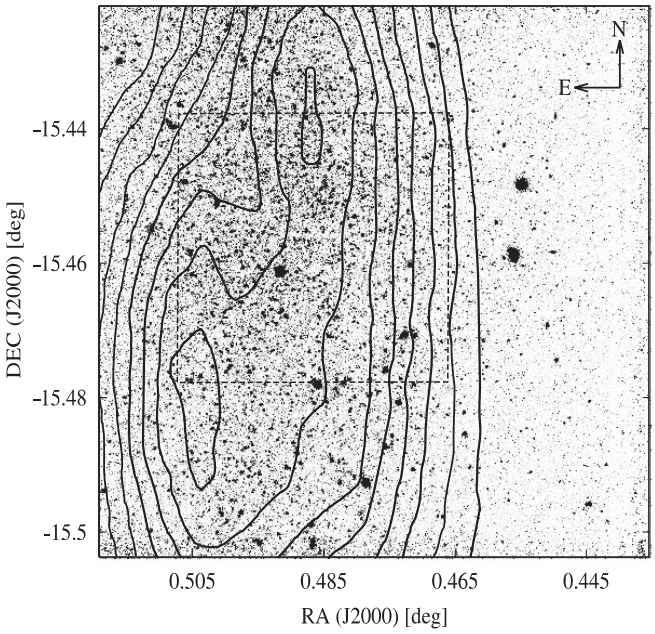

Fig. 1. Near-IR image of WLM. Isolines show the H I map of Jackson et al. (2004) at levels from 25 to 95 % of the maximum column density (2.16×10^{21} cm^{-2}), in increments of 10 %. The square marks the boundary of the "inner" field (see Sect. 2).

8×8 s exposures in K_S. The total integration time was 10 min in J_S (hereafter J for simplicity) and, in K_S, 21.33 min on the galaxy and 16 min on the "clear sky".

The data reduction followed the typical steps. First, we created a sky for each filter by median combination of the off-target images using suitable upper limits and rejection algorithms to exclude the stars present in the sky field. Next, we subtracted the sky from each image, and divided it by the dome flat. The dome flats are preferable in comparison to the sky flats because they allow us to remove the variable bias level, found in some Hawaii detectors. To account for the uneven illumination of the dome flat screen, we applied an illumination correction. It was derived from the photometry of a standard star, placed on 16 positions across the field of average view, in a 4×4 grid. Finally, the individual images were aligned and combined to form the final image (Fig. 1).

The photometric calibration was performed by comparing our instrumental photometry with the measurements from the 2MASS Point Source Catalog:

$$J = j - 5.55(\pm 0.05) \quad (1)$$

$$K_S = k - 8.65(\pm 0.18) \quad (2)$$

based on 18 common stars. Here J and K_S are the 2MASS systematic magnitudes, and j and k are the instrumental magnitudes. No statistically significant color terms were found.

The photometry was performed with the IRAF DAOPHOT package. In the galaxy field, 1550 stars were detected in J and 739 in K_S with a threshold of 4σ and 3σ, respectively, above the background. The instrumental magnitudes for each filter were obtained by using constant Gaussian PSF. The positions and magnitudes of all measured stars matched in both J and K_S frames with a maximum tolerance of 3 pixels (0.86 arcsec) are given in Table 1. The columns contain: identification number, RA and DEC (J2000), J and K_S magnitudes (the 1σ errors are

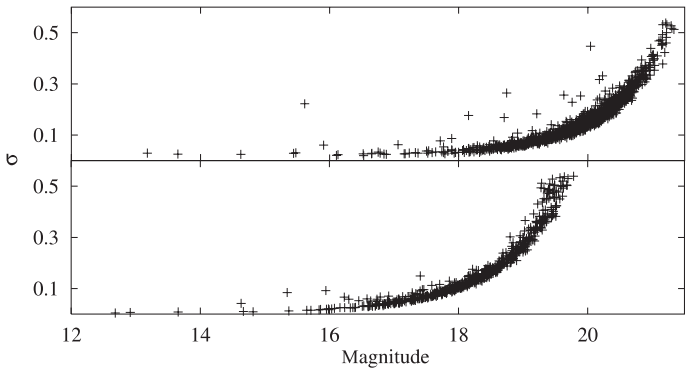

Fig. 2. Photometric errors as a function of the magnitude for the J- (*top*) and K_S- (*bottom*) bands. The completeness limits of our photometry are ~20.1 and ~17.9 mag for the J- and K_S-bands, respectively.

Table 1. Photometry of 555 WLM stars with J- and K_S-band photometry.

No	RA	Dec	J	K_S	Note
1	00:01:45.62	−15:30:06.6	19.713 (0.135)	18.268 (0.131)	M05 LC 120
2	00:01:46.86	−15:29:44.0	18.150 (0.047)	16.737 (0.058)	C
3	00:01:47.40	−15:29:49.1	19.762 (0.119)	18.376 (0.155)	C
4	00:01:47.50	−15:27:54.8	19.222 (0.073)	18.402 (0.140)	
5	00:01:47.99	−15:27:47.5	19.408 (0.092)	17.487 (0.065)	BD04
6	00:01:48.20	−15:26:49.0	19.327 (0.088)	17.855 (0.097)	C
7	00:01:48.34	−15:28:08.5	19.402 (0.107)	17.462 (0.096)	C
8	00:01:48.42	−15:27:08.6	19.078 (0.069)	18.273 (0.118)	
9	00:01:48.79	−15:27:35.2	19.800 (0.130)	18.849 (0.232)	
10	00:01:48.80	−15:27:16.8	19.132 (0.068)	18.037 (0.108)	BD04
11	00:01:49.09	−15:27:06.3	19.712 (0.109)	18.985 (0.255)	
12	00:01:49.11	−15:29:03.3	19.708 (0.114)	19.501 (0.418)	
13	00:01:49.26	−15:26:53.4	13.177 (0.029)	12.683 (0.004)	
14	00:01:49.33	−15:28:24.1	19.495 (0.092)	18.920 (0.253)	
15	00:01:49.50	−15:26:06.4	18.821 (0.056)	18.021 (0.103)	
16	00:01:49.56	−15:27:31.0	15.615 (0.222)	14.631 (0.042)	G
17	00:01:49.57	−15:28:00.6	18.921 (0.075)	17.781 (0.090)	
18	00:01:49.79	−15:29:42.1	19.211 (0.076)	18.764 (0.217)	
19	00:01:49.88	−15:26:32.3	18.833 (0.091)	17.404 (0.090)	C
20	00:01:49.94	−15:26:20.7	19.196 (0.076)	18.640 (0.192)	

The full table is available in the electronic edition.

given in brackets (keys to the notes: V - variable star, with identifier from the source paper (SC85 for Sandage & Carlson 1985 and M05 for Mora et al. in preparation), C - carbon star candidate (BD04 for Battinelli & Demers 2004), G - globular cluster). The paper edition of the journal contains only the first 20 entries. The rest of the table is available in the electronic version of the journal only. The measurement errors are plotted in Fig. 2.

The reduction and calibration procedures for the "clear sky" field follow analogous steps. The photometric equations obtained from 7 2MASS stars

$$J = j - 3.12(\pm 0.03) \quad (3)$$

$$K_S = k - 5.34(\pm 0.04) \quad (4)$$

were used to transform the magnitudes of 89 stars in J and 67 in K_S into 2MASS magnitudes. The matching procedure gives 50 common stars in J and K_S in total.

The luminosity functions in J and K_S are shown in Fig. 3. The number of stars in each bin is normalized to 1 square arcmin. We tested the completeness limit variations across the galaxy by splitting the field into an "inner" part, containing the area with maximum H I column densities, and an "outer" part, respectively

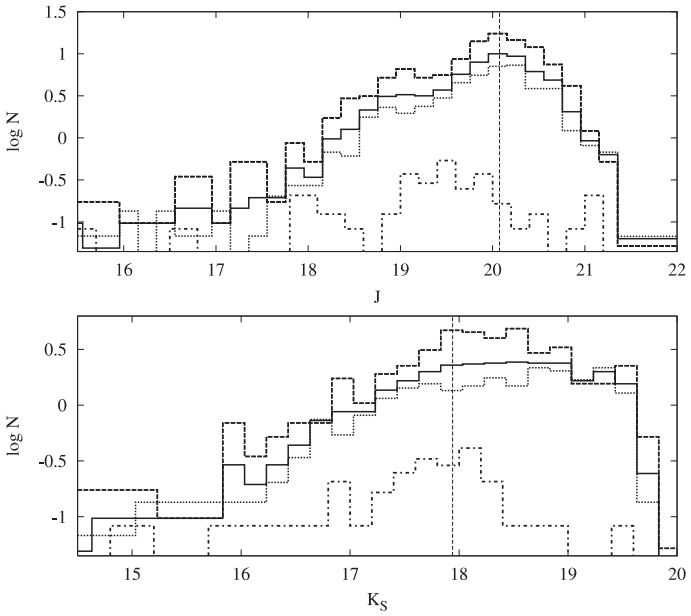

Fig. 3. Luminosity functions for J (*upper panel*) and K_S (*bottom panel*) with a magnitude bin of 0.2 mag. Log N is the number of stars normalized for 1 square arcmin. Each panel shows the luminosity functions for the whole field (solid lines), the inner part (dashed lines), and outer part (dotted lines). The LF for the "clear sky" field is also shown with dot-dashed lines. Vertical lines represent our galaxy 100% photometry completeness for every band.

5.76 and 14.77 square arcmin (see Fig. 1). The crowding effects are limited to ≤0.2 mag. We adopted $J^{\rm lim} \sim 20.1$ mag and $K_S^{\rm lim} \sim 17.9$ mag. For comparison the luminosity function of the "clear sky" is also shown in Fig. 3. On average the LF is nearly an order lower then the galaxy one.

3. Color–magnitude diagram

The color–magnitude diagram of WLM is shown in Fig. 4 (top panel). We used distance modulus $(m-M)_0 = 24.85$ mag – an average of the estimates of: (i) Minniti & Zijlstra (1997), who derived $(m-M)_0 = 24.75 \pm 0.1$ mag from the I-magnitude of the red giant branch (hereafter RGB) tip, and (ii) Rejkuba et al. (2000), who obtained $(m-M)_0 = 24.95 \pm 0.13$ mag from V-band photometry of the horizontal branch. These two values agree within the errors and they are derived from different methods and data sets. Corrections for the Galactic extinction were made using $E(B-V) = 0.037$ mag (Schlegel et al. 1998). Here and throughout the paper we use the extinction law of Rieke & Lebofsky (1985).

For the high Galactic latitude of WLM ($b = -73.62°$), we expect the foreground contamination to be negligible. This is confirmed from the number of stars found under similar observational conditions in our "clear sky", which is just 9% of all stars in the galaxy field. The color–magnitude diagram was constructed using the same distance modulus and Galactic extinction and is shown in Fig. 4 (right panel). In such way a true estimation of the Galaxy contamination can be made by counting the stars in 1 magnitude bins in M_{K_S}. The numbers are given on the right in Fig. 4 (left panel).

The comparison with isochrones of Bertelli et al. (1994) indicates that the majority of the stars are 1–10 Gyr old, with a significant population of AGB and carbon stars with $(J-K_S)_0 > 1$ mag. Only a handful of blue stars with $(J-K_S)_0 < 1$ mag and $M_{K_S} > -8$ mag are detected. We also identified a number of variable stars on our images from Sandage & Carlson (1985) and Mora et al. (in preparation). The RGB properties versus metallicity calibrations of Ivanov & Borissova (2002) predict that the RGB tip for the WLM metallicity is located at $M_{K_S} > -6.14$ mag. Unfortunately, the incompleteness of the photometry in this magnitude range prevents us from analysis of the RGB properties.

4. Carbon star identification and C/M ratio in the WLM

WLM is an unusually rich carbon star, along with two other dwarf galaxies – IC 1613 and NGC 6822 – according to Cook et al. (1986). Recently, Battinelli & Demers (2004) surveyed WLM using narrow band CN-TiO filters and identified 149 carbon stars and practically no M-type AGB stars (77 identified carbon stars in our field are marked in Table 1 with BD04). They also found an extremely high C/M ratio of WLM: 12.4 ± 3.7.

The IR photometry allows us to carry out an independent census of the carbon stars, following the method applied on the Magellanic Clouds (Cioni & Habing 2003), NGC 6822 (Cioni & Habing 2005, Kang et al. 2006), NGC 185 (Kang et al. 2005), and NGC 147 (Sohn et al. 2006). It is found that the color distribution of all AGB stars have a well-pronounced discontinuity at some point, M-type stars have a peak followed by a red tail of carbon stars. We separated the carbon-rich from the oxygen-rich stars using the color distribution of the stars above the RGB tip (Fig. 6, the inset) and found color limit at $(J-K_S)_0 = 1.20$ mag. A similar dereddened limit was found by Cioni & Habing (2005) for NGC 6822, and Sohn et al. (2006) for NGC 147: $(J-K_S)_0 = 1.24$ and $(J-K_S)_0 = 1.28$, respectively.

Integrating over the two parts of the histogram we obtain 146 carbon stars and 259 M stars. The latter number includes all stars with spectral types M0 and later (M0, M1, M2, etc.), which is sometimes designated as M0+. Using the same criteria on the "clear sky" field we obtain 31 C stars and 19 M stars as all of them are above the RGB tip. Taking into account the latter numbers, this will reduce our C stars to 115 and the M star to 240.

The K_S luminosity functions for our carbon star sample and for the 77 cross-identified carbon stars (shown in Fig. 6) from Battinelli & Demers (2004) are shown in Fig. 5. To eliminate the binning effects, we created two luminosity functions for each data set, shifting the bin centers by half of the bin width, and averaged them. We fitted the luminosity function with a Gaussian, in two iterations, excluding the values that deviated more than 3σ. The final fits have a mean of $\langle K_S \rangle = 17.35$ mag, $\sigma = 0.71$ mag for our sample and $\langle K_S \rangle = 17.33$ mag, $\sigma = 0.51$ mag for the 77 carbon stars from Battinelli & Demers (2004), which correspond to $\langle M_{K_S} \rangle = -7.51$ mag and $\langle M_{K_S} \rangle = -7.53$ mag, respectively.

Previous studies in some LG galaxies in the near IR lead to identical mean absolute K magnitude of the C stars: $\langle M_{K_S} \rangle = -7.93 \pm 0.36$ mag (Kang et al. 2005), $\langle M_{K_S} \rangle = -7.56 \pm 0.47$ mag (Sohn et al. 2006), and $\langle M_{K_S} \rangle = -7.60 \pm 0.50$ mag (Kang et al. 2006) for NGC 185, NGC 147 and NGC 6822, respectively. $\langle M_{K_S} \rangle$ in WLM is comparable with these values in 1σ level and support this assumption. The sample of galaxies includes dwarf irregulars and dwarf ellipticals, but is not representative of a wide range of metallicity and a possible influence over the mean absolute K magnitude cannot be entirely excluded.

Next, we derived a C/M ratio of 0.56 ± 0.12 (foreground corrected ratio 0.48), using the carbon and M-type stars we

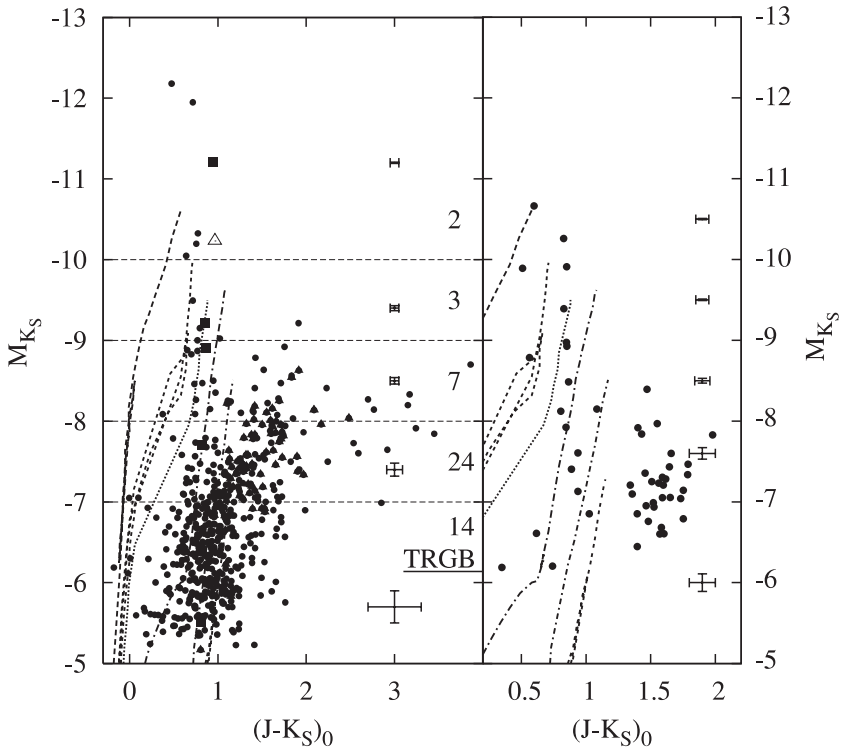

Fig. 4. Near-IR M_{K_S} versus $(J - K_S)_0$ mag color–magnitude diagram of WLM (*left panel*) and the "clear sky" field (*right panel*; see Sect. 3 for details). The typical measurement errors for stars with $(J - K_S)_0$ = 1 mag are shown on the right. Isochrones for the 10, 20, 30, 100 Myr, 1 and 10 Gyr, and Z=0.001 from Bertelli et al. (1994) are plotted. *Left panel*: the open triangle indicates the location of the WLM globular cluster. Six variable stars from Sandage & Carlson (1985) are plotted with solid squares and 77 carbon stars of Battinelli & Demers (2004) are shown with solid triangles. The level of the RGB tip is also marked on the right. The number of foreground stars in every 1-mag bin along M_{K_S} obtained from CMD of "clear sky" are given on the right.

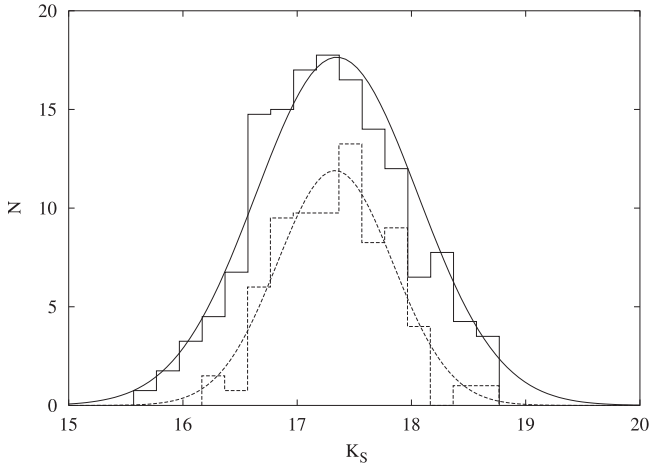

Fig. 5. Luminosity functions of the carbon stars in WLM. The solid line represents the distribution of carbon stars above the RGB tip. The dashed line shows the 77 carbon stars from Battinelli & Demers (2004) that we identified in our field. The bin width is 0.2 mag. The final Gaussian fits to the data are shown (see Sect. 4 for details).

identified above the RGB tip. However, Cioni & Habing (2005) pointed that this classification method omits the early-type carbon stars that might be bluer than the adopted color limit. The incompleteness due to this effect can be estimated by comparison of our carbon star list and that of Battinelli & Demers (2004) – it yielded additional 15 carbon stars among the M stars, bringing the C/M ratio up to 0.66 ± 0.11 (0.58). The difference between the two values is small, considering the Poisson uncertainties given here.

Both values obtained here are smaller by a factor of 20 than the result of Battinelli & Demers (2004): C/M0+∼12.4. The large difference is due to the presence of the M-type AGB population, which is almost entirely absent in Battinelli & Demers' (2004) survey of WLM. We can only speculate that this difference is related to the narrow-band filter centered at the TiO absorption feature – prominent for spectral types later than M3. Their method probably omits early M-type stars. Furthermore, the low metallicity of WLM additionally diminishes the TiO feature strength and makes the detection of M-type stars more difficult.

5. Spatial distribution of the stellar populations

Our data cover most of the main body of WLM, allowing us to study the spatial distribution of stellar populations. We created 2-dimensional histograms (Fig. 7) with 22.5×22.5 arcsec^2 bins, corresponding to a linear scale of 100×100 pc at the distance of the galaxy. The distributions were smoothed by a box-car function of width 2.

The histograms indicate no major difference between the stellar distributions. There are two peaks, corresponding to complexes with typical sizes of a few hundred parsecs. The C/M ratio exhibits a more complicated behavior – the peak is slightly offset from the peak of the stellar distributions. Further studies are necessary to verify if this reflects a real metallicity or an age gradient across the galaxy.

6. Miscellaneous

6.1. Cepheid distance to WLM in the near-IR

We identified 5 Cepheids from the list of Sandage & Carlson (1985) on our J-band image (the K_S image is too shallow to detect them). We derived a distance to WLM adopting the period–luminosity relation of Gieren et al. (1998):

$$M_J = -5.240(\pm 0.028) - 3.129(\pm 0.052) \times (\log P - 1.0), \qquad (5)$$

where M_J is the absolute J-band magnitude of the Cepheids and P is the period in days. The distances to individual Cepheids are listed in Table 2. The columns contain: identification number,

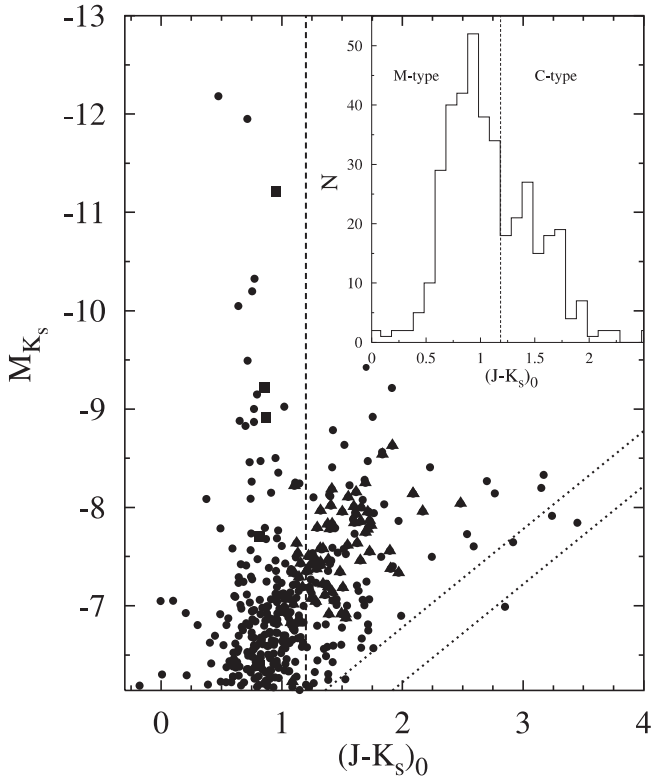

Fig. 6. Color–magnitude M_{K_S} versus $(J - K_S)_0$ diagram for AGB stars in WLM. The two dotted lines represent the 100% and 25% photometry completeness limits. Six variables from Sandage & Carlson (1985) are plotted with solid squares and 77 carbon stars from Battinelli & Demers (2004) are plotted with solid triangles. The inset is a color distribution of the stars above the RGB tip, used to separate the oxygen-rich and carbon-rich stars. See Sect. 4 for details. The separation line (dashed line) $(J - K_S)_0 = 1.20$ is shown on both panels.

J-band magnitude (the 1σ errors are given in brackets), period in days from Sandage & Carlson (1985), absolute magnitude calculates from Eq. (5), apparent distance modulus, total extinction in A_J derived from gas-to-dust ratio (including Milky Way extinction of $A_J = 0.033$ mag, Schlegel et al. 1998), and true distance modulus $(m - M)_0$. We removed the Milky Way extinction using $A_J = 0.033$ mag. To correct for the internal extinction towards individual Cepheids we used the H I map of Jackson et al. (2004). The hydrogen surface densities were converted into extinction, assuming the gas-to-dust ratio $N(\mathrm{H\,I})/E(B-V) = 60 \pm 10.0$ [10^{21} at. cm^{-2} mag^{-1}]. This value is an extrapolation based on a linear least-squares fit (Fig. 8) of the gas-to-dust ratio versus log(O/H)+12:

$$N(\mathrm{H\,I})/E(B-V) = -(58 \pm 5) \times [\log(\mathrm{O/H}) + 12] + (517 \pm 44), \quad (6)$$

with rms = 2.

This relation is based on gas-to-dust ratio estimates for: the solar neighborhood (Bohlin et al. 1978; marked MW in Fig. 8), the M 31 outskirts (Cuillandre et al. 2001; M 31$_o$), LMC (Junkkarinen et al. 2004; LMC), and SMC (Jakobsson et al. 2004; SMC). The abundances are taken from Russell & Dopita (1990) for LMC and SMC. In the case of the Milky Way we used the Galactic metallicity gradient from Esteban et al. (2005), and for M 31 – the metallicity gradient of Smartt et al. (2001). Note that this is a preliminary calibration, based on a limited number of measurements. More gas-to-dust ratios are necessary to derive a reliable relation. Finally, we assumed that the Cepheids are located on the WLM mid-plane and therefore, the extinctions are due to only half of the total hydrogen column densities. The extinction intrinsic to WLM does not exceed 0.015 mag, due to the high gas-to-dust ratio of the galaxy.

Table 2. Cepheid distance to WLM.

No	J	Period, days	M_J	$(m-M)_J$	A_J	$(m-M)_0$
7	20.108 (0.155)	7.6712	–4.880	24.988	0.048	24.940
8	20.016 (0.150)	7.3754	–4.827	24.843	0.047	24.796
21	19.829 (0.124)	9.33306	–5.146	24.975	0.044	24.931
48	19.724 (0.160)	8.53000	–5.024	24.748	0.048	24.700
66	20.197 (0.189)	4.54714	–4.170	24.367	0.040	24.327

Rejecting the outlier No. 66 (see Table 2), we obtain a median distance modulus of $(m - M)_0 = 24.84 \pm 0.14$ mag. We tentatively assume that the error is given by the maximum deviation. In addition, there are systematic errors of 0.03 mag for the zero-point of the period–luminosity relation (Eq. (5)), and 0.02 mag for the LMC distance adopted in Gieren et al. (1998).

6.2. Variable stars in WLM

Some variable stars from the lists of Sandage & Carlson (1985) and Mora et al. (in preparation) were included in our field. They are marked in Table 1.

6.3. Structural parameters of WLM

Structural parameters of galaxies are determined more reliably from IR images rather than optical ones because the effects of the intrinsic extinction are diminished. Our images do not encompass the entire galaxy, but nevertheless we are able to approximately determine the scale length along the major axis. To do that we averaged the pixel values in a 63.4-arcsec wide strip (~300 pc at the distance of WLM), crossing the center of the galaxy in a North-South direction. We used the J-band image because of the higher signal-to-noise ratio. The average flux values along the semi-major axis are shown in Fig. 9. An exponential law fit over the central 1 kpc region of WLM yielded a scale length of 0.75 ± 0.14 kpc, similar to the scale length of 0.9 kpc determined by Fisher & Tully (1975). The inset in Fig. 9 shows histograms of the scale lengths for dwarf galaxies in the Local Group from the compilation of Mateo (1998).

The bright – and younger – stars in the galaxy are resolved on our images, but the fainter – and older ones – are not. We addressed the question if there is a different scale length for different stellar populations by excluding the bright stars from this analysis: we averaged the J-band image with a 61×61 pixel median filter, effectively removing the resolved stars. The derived scale length for the "older" population was 0.71 ± 0.04 kpc, again for the central 1 kpc of the galaxy. Our estimates have to be treated with caution because the strip is not perfectly aligned along the major axis.

7. Discussion and summary

This work adds another object to the list of galaxies with homogeneously determined C/M0+ ratios from near-IR photometry: LMC, SMC, NGC 6822, NGC 147, NGC 185 and now the WLM. This is an opportunity for an independent check of the results from narrow-band carbon star surveys. The number of data points is still limited and did not allow us to test if using only C/M ratios derived from IR observations can reduce the spread of the relation but this is the objective of our further studies.

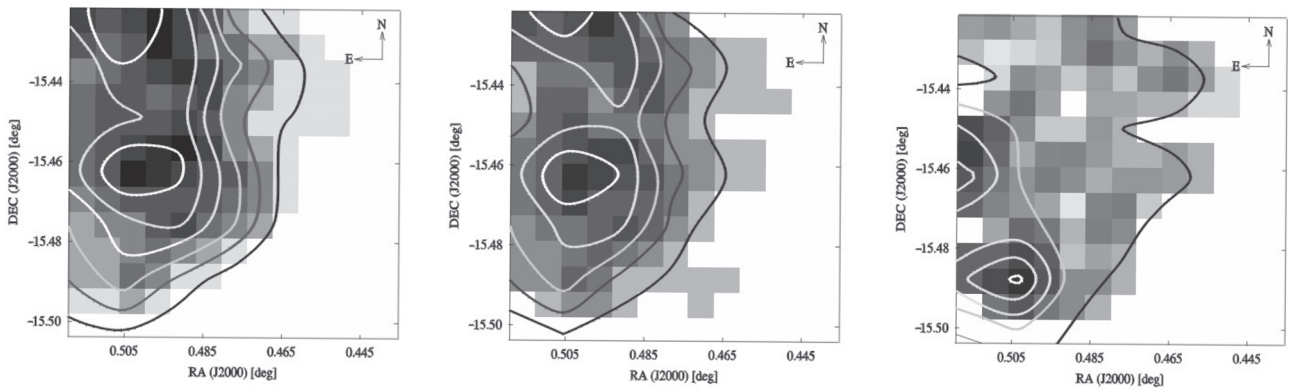

Fig. 7. Spatial distribution of all stars (*left*), AGB stars (*middle*), and C/M ratio (*right panel*). The isolines are at levels: 1 to 6 with a step of 1, 1 to 5 with a step of 1, and 0.2 to 1.4 with a step of 0.3, respectively, for the three plots from left to right.

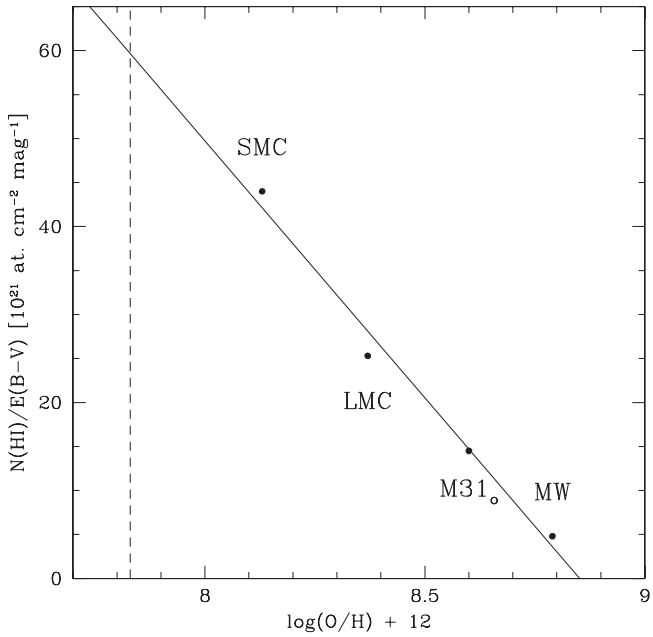

Fig. 8. Gas-to-dust ratio versus log(O/H)+12 relation. Data points are labeled (see Sect. 6.1 for details). The solid line is the linear least-squares fit, and the vertical dashed line indicates the WLM abundance from Lee et al. (2005).

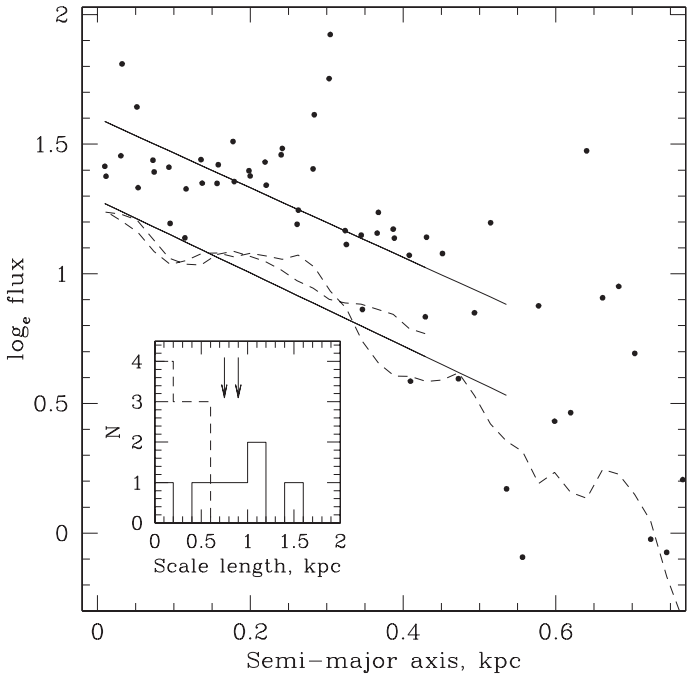

Fig. 9. Scale length of the WLM disk in *J*-band. The dots indicate the average values along the semi-major axis, the dashed line is the same for the median-averaged image. The solid lines are the fits. The inset shows the distribution of the scale lengths for the dwarf irregulars (solid line) and dwarf spheroidal galaxies (dashed lines) in the Local Group. The left arrow indicates our estimate and the right arrow shows the estimate of Fisher & Tully (1975).

We obtained a C/M ratio of ∼0.6 ± 0.1 and a peak of the carbon stars luminosity function of $\langle M_{K_S} \rangle = -7.51$ mag for the WLM.

To measure the intrinsic reddening in WLM we used the H I map of WLM (Jackson et al. 2004), and we adopted a linear dependence of the gas-to-dust ratio on the metallicity: $N(\mathrm{H\,I})/E(B-V) = -(58 \pm 5) \times [\log(\mathrm{O/H})+12] + (517 \pm 44)$. The gas-to-dust ratio for the WLM is 60 ± 10 [10^{21} at. cm^{-2} mag^{-1}]. This allows us to measure the extinction along the line of sight towards individual Cepheids and by the period–luminosity relation for the Cepheids (Gieren 1998), in the IR we determined the distance to the WLM – $(m - M)_0 = 24.84 \pm 0.14$ mag, similar to the previous estimates. To probe the significance of the used PL relation, we re-determined the distance modulus using the PL relation calibrated by Testa et al. (2006) for the Cepheids in two LMC young clusters. This results in a distance modulus between 24.76 and 25.00, depending on the assumed pulsation models. Finally, we fitted the surface brightness distribution along the main axis of WLM with an exponential law yielding a scale length of 0.75 ± 0.14 kpc, a typical value for the dwarf irregular galaxies.

Acknowledgements. This work obtained limited support by the grants F-1302/03 and VU-F-201/06 of the Bulgarian Scientific Foundation. Also, this publication makes use of data products from the Two Micron All Sky Survey, which is a joint project of the University of Massachusetts and the IR Processing and Analysis Center/California Institute of Technology, funded by the National Aeronautics and Space Administration and the National Science Foundation. This research has made use of the SIMBAD database, operated at CDS, Strasbourg, France. The authors thank Dr. M.-R. Cioni for the useful comments and the anonymous referee for the help in improving the article.

References

Ables, H. D., & Ables, P. G. 1977, ApJS, 34, 245
Albert, L., Demers, S., & Kunkel, W. E. 2000, ApJ, 119, 2780

Battinelli, P., & Demers, S. 2004, A&A, 416, 111
Battinelli, P., & Demers, S. 2005, A&A, 434, 657
Bertelli, G., Bressan, A., Chiosi, C., Fagotto, F., & Nasi, E. 1994, A&AS, 106, 275
Bohlin, R., Savage, B.,& Drake, J. 1978, ApJ, 224, 132
Cioni, M.-R. L., & Habing, H. J. 2003, A&A, 402, 133
Cioni, M.-R. L., & Habing, H. J. 2005, A&A, 429, 837
Cook, K. H., Aaronson, M., & Norris, J. 1986, ApJ, 305, 634
Cuillandre, J., Lequeux, J., Allen, R. J., Mellier, Y., Bertin, E. 2001, ApJ, 554, 190
Dolphin, A. E. 2000, ApJ, 531, 804
Esteban, C., García-Rojas, J., Peimbert, M., et al. 2005, ApJS, 618, 95
Ferraro, F. R., Fusi Pecci, F., Tosi, M., & Buonanno, R. 1989, MNRAS, 241, 433
Fisher, J. R., & Tully, R. B. 1975, A&A, 44, 151
Gieren, W. P., Fouque, P., & Gomez, M. 1998, ApJ, 496, 17
Groenewegen, M. A. T. 2006, pnbm.conf., 108
Hodge, P. W., Dolphin, A. E., Smith, R. T., & Mateo, M. 1999, ApJ, 521, 577
Iben, I. & Renzini, A. 1983, ARA&A, 21, 271
Ivanov, V. D., & Borissova, J. 2002, 390, 937
Jackson, D. C., Skillman, E. D., Cannon, J. M., & Côté, S. 2004, AJ, 128, 1219
Jakobsson, P., Hjorth, J., Fynbo, J. P. U., et al. 2004, A&A, 427, 785
Junkkarinen, V., Cohen, R., Ross, D., et al. 2004, ApJ, 614, 658
Lee, H., Skillman, E. D., & Venn, K. A. 2005, ApJ, 620, 223
Kang, A., Sohn, Y.-J., Rhee, J., et al. 2005, A&A, 437, 61
Kang, A., Sohn, Y.-J., Kim, H.-I., et al. 2006, A&A, 454, 727
Mateo, M. 1998, ARA&A, 36, 435
Melotte, P. J. 1926, MNRAS, 86, 636
Minniti, D., & Zijlstra, A. A. 1997, AJ, 114, 147
Mora, M., Minniti, D., Catelan, M., Zijlstra, A., & Rejkuba, M. 2007, A&A, in preparation
Rejkuba, M., Minniti, D., Gregg, M. D., et al. 2000 ApJ, 120, 801
Rieke, G. M., & Lebofsky, M. J. 1985, ApJ, 288, 618
Russell, S. C., & Dopita, M. A. 1990, ApJS, 74, 93
Sandage, A., & Carlson, G. 1985, AJ, 90, 1464
Scalo. J. M., & Miller, G. E. 1981, ApJ, 248, L65
Schlegel, D. J., Frankbeiner, D. P., & Davis, M. 1998, ApJ, 500, 525
Smartt, S., Crowther, P., Dufton, P., et al. 2001, MNRAS, 325, 257
Sohn, Y.-J., Kang, A., Rhee, J., et al. 2006, ApJ, 445, 69
Testa, V., Ferraro, F. R., Ripepi, V., et al. 2006, MmSAI, 77, 263
Venn, K. A., Tolstoy, E., Kaufer, A., et al. 2003, AJ, 126, 1326
Wolf, M. 1909, Astron. Nachr., 183, 187

Online Material

Table 1. Photometry of 555 WLM stars with J- and K_S-band photometry (see Sect. 2 for details).

No	RA	Dec	J	K_S	Note
1	00:01:45.62	−15:30:06.6	19.713 (0.135)	18.268 (0.131)	M05 LC 120
2	00:01:46.86	−15:29:44.0	18.150 (0.047)	16.737 (0.058)	C
3	00:01:47.40	−15:29:49.1	19.762 (0.119)	18.376 (0.155)	C
4	00:01:47.50	−15:27:54.8	19.222 (0.073)	18.402 (0.140)	
5	00:01:47.99	−15:27:47.5	19.408 (0.092)	17.487 (0.065)	BD04
6	00:01:48.20	−15:26:49.0	19.327 (0.088)	17.855 (0.097)	C
7	00:01:48.34	−15:28:08.5	19.402 (0.107)	17.462 (0.096)	C
8	00:01:48.42	−15:27:08.6	19.078 (0.069)	18.273 (0.118)	
9	00:01:48.79	−15:27:35.2	19.800 (0.130)	18.849 (0.232)	
10	00:01:48.80	−15:27:16.8	19.132 (0.068)	18.037 (0.108)	BD04
11	00:01:49.09	−15:27:06.3	19.712 (0.109)	18.985 (0.255)	
12	00:01:49.11	−15:29:03.3	19.708 (0.114)	19.501 (0.418)	
13	00:01:49.26	−15:26:53.4	13.177 (0.029)	12.683 (0.004)	
14	00:01:49.33	−15:28:24.1	19.495 (0.092)	18.920 (0.253)	
15	00:01:49.50	−15:26:06.4	18.821 (0.056)	18.021 (0.103)	
16	00:01:49.56	−15:27:31.0	15.615 (0.222)	14.631 (0.042)	G
17	00:01:49.57	−15:28:00.6	18.921 (0.075)	17.781 (0.090)	
18	00:01:49.79	−15:29:42.1	19.211 (0.076)	18.764 (0.217)	
19	00:01:49.88	−15:26:32.3	18.833 (0.091)	17.404 (0.090)	C
20	00:01:49.94	−15:26:20.7	19.196 (0.076)	18.640 (0.192)	
21	00:01:50.10	−15:26:25.5	18.590 (0.053)	18.563 (0.172)	
22	00:01:50.31	−15:26:34.8	19.815 (0.116)	18.808 (0.223)	
23	00:01:50.56	−15:28:30.7	18.327 (0.045)	16.757 (0.034)	BD04
24	00:01:50.67	−15:27:31.9	19.120 (0.082)	17.820 (0.084)	BD04
25	00:01:50.68	−15:28:16.7	18.818 (0.078)	17.285 (0.075)	C
26	00:01:50.83	−15:25:33.6	19.773 (0.126)	18.734 (0.240)	
27	00:01:50.84	−15:29:47.0	18.855 (0.049)	17.596 (0.074)	C
28	00:01:50.85	−15:26:51.4	18.992 (0.062)	17.934 (0.092)	BD04
29	00:01:51.01	−15:26:14.4	18.235 (0.034)	17.572 (0.071)	
30	00:01:51.02	−15:27:00.0	19.603 (0.098)	18.085 (0.112)	C
31	00:01:51.13	−15:26:08.1	19.519 (0.108)	18.930 (0.262)	
32	00:01:51.14	−15:30:08.3	19.340 (0.118)	17.619 (0.096)	C
33	00:01:51.15	−15:26:33.8	19.423 (0.110)	17.864 (0.099)	C
34	00:01:51.17	−15:25:57.7	19.778 (0.132)	18.743 (0.201)	
35	00:01:51.17	−15:27:13.1	18.922 (0.068)	17.671 (0.073)	C
36	00:01:51.33	−15:29:13.2	20.066 (0.145)	19.286 (0.337)	
37	00:01:51.38	−15:27:37.5	19.906 (0.145)	19.070 (0.270)	
38	00:01:51.38	−15:29:06.6	16.753 (0.033)	16.035 (0.020)	
39	00:01:51.40	−15:28:55.2	18.536 (0.045)	17.075 (0.056)	C
40	00:01:51.48	−15:28:37.5	19.776 (0.130)	19.001 (0.263)	
41	00:01:51.53	−15:28:50.4	19.572 (0.098)	18.812 (0.208)	
42	00:01:51.56	−15:28:10.2	18.777 (0.062)	18.002 (0.106)	
43	00:01:51.67	−15:25:36.3	19.515 (0.093)	17.528 (0.065)	BD04
44	00:01:51.75	−15:27:40.3	19.117 (0.080)	18.256 (0.124)	
45	00:01:52.02	−15:28:56.5	19.692 (0.110)	18.824 (0.231)	
46	00:01:52.11	−15:26:29.7	18.951 (0.062)	18.000 (0.105)	
47	00:01:52.20	−15:29:50.8	19.494 (0.104)	17.803 (0.090)	C
48	00:01:52.23	−15:25:19.0	19.065 (0.078)	17.865 (0.113)	
49	00:01:52.23	−15:28:17.2	19.973 (0.145)	17.966 (0.104)	C
50	00:01:52.33	−15:26:07.5	19.867 (0.128)	19.471 (0.393)	
51	00:01:52.33	−15:27:59.7	19.239 (0.066)	18.510 (0.163)	
52	00:01:52.38	−15:29:50.5	18.643 (0.050)	16.911 (0.040)	BD04
53	00:01:52.42	−15:25:55.2	18.831 (0.061)	17.118 (0.046)	BD04
54	00:01:52.47	−15:25:39.2	18.152 (0.176)	16.300 (0.058)	C
55	00:01:52.53	−15:28:47.7	19.924 (0.139)	19.274 (0.365)	
56	00:01:52.57	−15:26:20.8	18.428 (0.052)	16.908 (0.039)	BD04
57	00:01:52.57	−15:27:02.8	19.822 (0.134)	18.755 (0.209)	
58	00:01:52.73	−15:26:38.8	19.123 (0.092)	17.962 (0.123)	
59	00:01:52.78	−15:28:07.8	19.986 (0.146)	18.899 (0.255)	
60	00:01:52.80	−15:26:26.0	19.585 (0.100)	18.682 (0.199)	
61	00:01:52.85	−15:27:28.3	18.994 (0.076)	18.039 (0.103)	
62	00:01:52.94	−15:26:46.8	19.235 (0.085)	18.573 (0.165)	
63	00:01:52.94	−15:27:49.4	19.454 (0.107)	18.523 (0.167)	
64	00:01:52.98	−15:28:56.8	19.457 (0.084)	18.990 (0.275)	
65	00:01:53.12	−15:29:22.1	19.355 (0.082)	18.674 (0.187)	

Table 1. continued.

No	RA	Dec	J	K_S	Note
66	00:01:53.17	−15:28:14.1	16.650 (0.026)	15.862 (0.018)	
67	00:01:53.22	−15:28:40.3	17.830 (0.036)	17.816 (0.091)	
68	00:01:53.27	−15:29:25.6	17.155 (0.026)	16.403 (0.026)	
69	00:01:53.28	−15:26:33.7	19.033 (0.068)	18.155 (0.118)	
70	00:01:53.32	−15:26:43.8	18.895 (0.063)	17.895 (0.086)	
71	00:01:53.39	−15:27:07.4	18.923 (0.060)	17.807 (0.085)	
72	00:01:53.45	−15:28:33.4	19.831 (0.134)	18.538 (0.165)	C
73	00:01:53.54	−15:28:13.7	17.765 (0.053)	16.228 (0.066)	C
74	00:01:53.54	−15:29:16.7	19.434 (0.088)	18.808 (0.230)	
75	00:01:53.55	−15:27:16.5	18.765 (0.044)	17.870 (0.093)	
76	00:01:53.55	−15:30:04.9	19.158 (0.069)	17.996 (0.111)	
77	00:01:53.57	−15:27:55.2	18.905 (0.057)	18.136 (0.114)	
78	00:01:53.62	−15:28:23.0	17.891 (0.042)	17.281 (0.055)	
79	00:01:53.66	−15:28:19.4	20.518 (0.222)	19.506 (0.382)	
80	00:01:53.67	−15:28:21.0	20.209 (0.202)	18.949 (0.244)	
81	00:01:53.70	−15:28:37.2	18.120 (0.039)	17.440 (0.063)	
82	00:01:53.71	−15:28:15.3	19.235 (0.081)	18.390 (0.148)	
83	00:01:53.77	−15:28:50.1	15.441 (0.028)	14.667 (0.010)	
84	00:01:53.83	−15:26:39.9	16.655 (0.028)	15.984 (0.020)	
85	00:01:53.83	−15:29:39.7	19.684 (0.121)	18.822 (0.221)	
86	00:01:53.87	−15:27:03.5	19.664 (0.119)	19.219 (0.341)	
87	00:01:53.90	−15:28:18.5	19.249 (0.064)	17.810 (0.085)	C
88	00:01:53.94	−15:27:01.7	19.380 (0.086)	18.516 (0.167)	
89	00:01:53.96	−15:26:34.8	18.964 (0.067)	17.849 (0.101)	BD04
90	00:01:54.02	−15:29:12.1	19.092 (0.071)	16.905 (0.042)	BD04
91	00:01:54.03	−15:28:39.2	19.411 (0.102)	19.220 (0.326)	
92	00:01:54.04	−15:29:07.6	18.171 (0.037)	16.749 (0.050)	C
93	00:01:54.06	−15:25:31.1	19.299 (0.076)	17.658 (0.094)	C
94	00:01:54.10	−15:27:25.3	19.785 (0.141)	18.052 (0.105)	C
95	00:01:54.13	−15:25:55.8	19.876 (0.112)	18.436 (0.142)	C
96	00:01:54.15	−15:25:37.9	20.154 (0.161)	18.609 (0.185)	C
97	00:01:54.16	−15:28:01.5	19.772 (0.132)	18.847 (0.218)	
98	00:01:54.19	−15:28:15.6	19.236 (0.080)	18.434 (0.158)	
99	00:01:54.25	−15:28:32.3	15.476 (0.030)	14.817 (0.009)	
100	00:01:54.27	−15:29:13.8	18.221 (0.050)	16.639 (0.051)	C
101	00:01:54.28	−15:28:22.2	19.198 (0.096)	18.165 (0.115)	
102	00:01:54.31	−15:27:53.1	18.761 (0.058)	17.779 (0.084)	
103	00:01:54.41	−15:26:30.3	18.766 (0.056)	18.079 (0.106)	
104	00:01:54.42	−15:27:18.0	18.325 (0.053)	16.613 (0.032)	BD04
105	00:01:54.48	−15:27:46.5	19.059 (0.080)	18.204 (0.126)	
106	00:01:54.53	−15:26:21.8	19.923 (0.141)	18.839 (0.216)	
107	00:01:54.53	−15:28:44.0	18.830 (0.067)	18.167 (0.133)	
108	00:01:54.57	−15:27:54.8	18.867 (0.067)	17.677 (0.079)	BD04
109	00:01:54.65	−15:27:47.5	20.079 (0.157)	19.499 (0.418)	
110	00:01:54.66	−15:26:04.2	18.620 (0.055)	17.282 (0.057)	BD04
111	00:01:54.71	−15:26:07.4	18.652 (0.050)	17.673 (0.080)	
112	00:01:54.71	−15:26:23.5	19.668 (0.114)	18.301 (0.133)	C
113	00:01:54.71	−15:26:26.6	18.857 (0.072)	17.438 (0.065)	C
114	00:01:54.76	−15:26:53.9	19.344 (0.095)	18.294 (0.136)	
115	00:01:54.80	−15:28:37.0	18.841 (0.058)	17.945 (0.097)	
116	00:01:54.81	−15:28:17.5	18.759 (0.055)	17.443 (0.064)	BD04
117	00:01:54.87	−15:28:46.2	18.805 (0.057)	17.073 (0.059)	C
118	00:01:54.89	−15:27:52.4	19.896 (0.132)	18.985 (0.262)	
119	00:01:54.89	−15:28:55.4	19.610 (0.106)	18.841 (0.215)	
120	00:01:54.98	−15:29:32.5	17.715 (0.077)	15.943 (0.092)	C
121	00:01:55.04	−15:26:52.1	20.067 (0.157)	19.437 (0.409)	
122	00:01:55.04	−15:28:18.7	18.573 (0.051)	17.594 (0.069)	
123	00:01:55.05	−15:26:04.7	19.684 (0.139)	18.836 (0.256)	
124	00:01:55.05	−15:27:20.5	18.692 (0.060)	17.914 (0.097)	
125	00:01:55.08	−15:26:49.1	19.513 (0.098)	18.628 (0.208)	
126	00:01:55.10	−15:27:01.1	19.835 (0.131)	16.666 (0.030)	C
127	00:01:55.11	−15:25:54.5	20.179 (0.150)	19.348 (0.376)	SC85 V15
128	00:01:55.16	−15:29:49.2	19.436 (0.091)	18.053 (0.120)	C

Table 1. continued.

No	RA	Dec	J	K_S	Note
129	00:01:55.20	−15:26:22.0	20.209 (0.161)	16.950 (0.041)	C
130	00:01:55.26	−15:26:06.2	18.879 (0.056)	17.794 (0.084)	
131	00:01:55.30	−15:25:51.8	19.738 (0.099)	19.023 (0.266)	
132	00:01:55.37	−15:27:10.6	17.370 (0.029)	16.600 (0.029)	
133	00:01:55.38	−15:27:31.8	19.012 (0.077)	18.426 (0.170)	
134	00:01:55.39	−15:28:06.7	19.047 (0.074)	18.129 (0.113)	
135	00:01:55.39	−15:28:47.3	19.381 (0.095)	18.068 (0.116)	C
136	00:01:55.42	−15:29:29.4	18.456 (0.045)	17.948 (0.109)	
137	00:01:55.44	−15:26:54.6	19.105 (0.069)	18.134 (0.107)	
138	00:01:55.47	−15:25:52.1	17.644 (0.034)	16.714 (0.033)	
139	00:01:55.50	−15:27:15.6	17.535 (0.038)	16.775 (0.037)	
140	00:01:55.50	−15:27:25.4	19.421 (0.095)	18.539 (0.179)	
141	00:01:55.53	−15:26:17.1	18.501 (0.046)	17.083 (0.044)	BD04
142	00:01:55.53	−15:26:48.3	18.609 (0.059)	17.433 (0.059)	BD04
143	00:01:55.53	−15:28:53.4	18.075 (0.043)	17.186 (0.048)	
144	00:01:55.56	−15:27:37.1	19.123 (0.068)	18.140 (0.116)	
145	00:01:55.56	−15:28:54.7	19.553 (0.103)	18.591 (0.181)	
146	00:01:55.58	−15:28:37.7	18.207 (0.042)	17.390 (0.062)	
147	00:01:55.60	−15:27:47.1	19.242 (0.073)	18.640 (0.191)	
148	00:01:55.60	−15:27:53.4	19.675 (0.134)	19.279 (0.355)	
149	00:01:55.62	−15:25:27.7	19.653 (0.137)	18.864 (0.270)	
150	00:01:55.62	−15:30:01.5	19.821 (0.142)	19.292 (0.361)	
151	00:01:55.69	−15:27:02.3	18.736 (0.056)	17.574 (0.068)	BD04
152	00:01:55.71	−15:26:24.6	19.022 (0.057)	17.521 (0.063)	BD04
153	00:01:55.77	−15:28:39.4	16.783 (0.029)	15.995 (0.017)	
154	00:01:55.79	−15:29:22.6	20.316 (0.241)	18.803 (0.228)	
155	00:01:55.81	−15:25:56.4	18.728 (0.052)	17.498 (0.070)	BD04
156	00:01:55.83	−15:28:12.7	19.593 (0.116)	18.599 (0.177)	
157	00:01:55.86	−15:27:30.2	19.089 (0.067)	18.477 (0.144)	
158	00:01:55.87	−15:25:31.4	19.538 (0.136)	18.837 (0.225)	
159	00:01:55.89	−15:29:04.7	18.291 (0.042)	17.631 (0.081)	
160	00:01:55.93	−15:29:33.0	19.060 (0.074)	18.211 (0.143)	
161	00:01:55.94	−15:26:44.5	18.468 (0.055)	17.032 (0.045)	BD04
162	00:01:56.00	−15:27:03.5	19.050 (0.070)	17.979 (0.114)	
163	00:01:56.00	−15:28:44.6	19.199 (0.080)	18.585 (0.169)	
164	00:01:56.01	−15:28:04.3	19.887 (0.253)	18.667 (0.205)	C
165	00:01:56.02	−15:25:57.0	19.651 (0.105)	18.810 (0.210)	
166	00:01:56.10	−15:26:42.6	19.850 (0.151)	18.114 (0.125)	C
167	00:01:56.10	−15:29:06.2	18.708 (0.061)	17.447 (0.063)	BD04
168	00:01:56.12	−15:28:05.8	19.055 (0.072)	17.789 (0.097)	BD04
169	00:01:56.16	−15:27:10.3	19.148 (0.072)	18.636 (0.186)	
170	00:01:56.18	−15:29:21.2	18.800 (0.054)	18.263 (0.149)	
171	00:01:56.21	−15:27:35.8	18.641 (0.055)	17.020 (0.047)	BD04
172	00:01:56.27	−15:27:51.5	19.902 (0.139)	18.899 (0.209)	
173	00:01:56.28	−15:26:35.7	17.588 (0.031)	17.077 (0.042)	
174	00:01:56.28	−15:28:14.8	19.061 (0.069)	18.144 (0.147)	
175	00:01:56.29	−15:26:45.6	18.790 (0.069)	17.948 (0.096)	
176	00:01:56.29	−15:29:17.8	18.915 (0.064)	17.992 (0.102)	
177	00:01:56.34	−15:25:26.5	20.146 (0.177)	19.269 (0.445)	
178	00:01:56.34	−15:28:14.8	18.775 (0.057)	17.868 (0.111)	
179	00:01:56.37	−15:28:49.9	19.488 (0.094)	18.496 (0.172)	
180	00:01:56.39	−15:25:50.1	19.564 (0.108)	19.261 (0.338)	
181	00:01:56.39	−15:26:49.7	19.759 (0.124)	18.881 (0.228)	
182	00:01:56.41	−15:25:52.5	19.404 (0.101)	18.593 (0.169)	
183	00:01:56.43	−15:28:52.3	19.920 (0.134)	19.053 (0.296)	
184	00:01:56.44	−15:28:47.2	18.679 (0.051)	17.006 (0.041)	BD04
185	00:01:56.45	−15:25:22.8	18.741 (0.074)	17.516 (0.078)	BD04
186	00:01:56.45	−15:27:03.7	18.516 (0.049)	18.676 (0.201)	
187	00:01:56.45	−15:27:08.3	19.401 (0.099)	18.932 (0.248)	
188	00:01:56.49	−15:25:45.9	19.876 (0.137)	19.624 (0.493)	
189	00:01:56.52	−15:26:02.8	19.912 (0.127)	19.152 (0.290)	
190	00:01:56.54	−15:27:39.9	19.792 (0.102)	18.830 (0.235)	
191	00:01:56.62	−15:26:42.3	18.970 (0.070)	18.002 (0.113)	
192	00:01:56.64	−15:27:48.1	19.358 (0.100)	17.948 (0.102)	BD04
193	00:01:56.67	−15:28:31.8	18.567 (0.059)	17.990 (0.112)	
194	00:01:56.68	−15:25:47.0	18.586 (0.049)	17.491 (0.068)	

Table 1. continued.

No	RA	Dec	J	K_S	Note
195	00:01:56.68	−15:27:41.9	19.428 (0.099)	18.451 (0.162)	
196	00:01:56.69	−15:28:03.9	18.380 (0.048)	18.059 (0.124)	
197	00:01:56.72	−15:28:17.5	19.035 (0.065)	18.434 (0.175)	
198	00:01:56.73	−15:26:03.7	18.810 (0.065)	18.062 (0.111)	
199	00:01:56.73	−15:28:40.5	14.625 (0.024)	13.656 (0.008)	SC85 28 LC
200	00:01:56.74	−15:26:58.6	18.809 (0.061)	18.112 (0.123)	
201	00:01:56.78	−15:27:09.2	19.321 (0.093)	18.398 (0.147)	
202	00:01:56.86	−15:28:38.0	19.879 (0.147)	18.196 (0.126)	C
203	00:01:56.87	−15:27:10.7	18.575 (0.056)	17.892 (0.101)	
204	00:01:56.87	−15:28:50.1	17.500 (0.037)	16.510 (0.030)	
205	00:01:56.89	−15:25:26.2	18.370 (0.045)	17.228 (0.067)	BD04
206	00:01:56.90	−15:27:05.4	19.360 (0.080)	19.178 (0.286)	
207	00:01:56.90	−15:28:30.3	19.135 (0.072)	18.365 (0.129)	
208	00:01:56.92	−15:26:12.3	18.693 (0.057)	17.921 (0.095)	
209	00:01:56.94	−15:30:05.3	17.581 (0.050)	15.649 (0.059)	C
210	00:01:56.99	−15:29:55.4	16.131 (0.023)	17.407 (0.149)	SC85 11 LC
211	00:01:57.03	−15:28:22.6	18.801 (0.053)	18.570 (0.168)	
212	00:01:57.05	−15:26:38.0	18.699 (0.053)	17.908 (0.104)	
213	00:01:57.05	−15:27:50.2	19.361 (0.089)	19.268 (0.340)	
214	00:01:57.08	−15:29:07.9	19.609 (0.127)	18.528 (0.181)	
215	00:01:57.10	−15:26:17.6	17.329 (0.031)	16.362 (0.025)	
216	00:01:57.12	−15:27:17.3	19.847 (0.131)	18.848 (0.257)	
217	00:01:57.19	−15:28:35.5	19.349 (0.088)	18.643 (0.180)	
218	00:01:57.20	−15:26:43.9	18.881 (0.063)	18.248 (0.128)	
219	00:01:57.20	−15:27:10.5	19.199 (0.089)	18.584 (0.177)	
220	00:01:57.22	−15:27:22.8	19.789 (0.118)	18.780 (0.218)	
221	00:01:57.27	−15:26:08.2	18.901 (0.060)	18.003 (0.108)	
222	00:01:57.33	−15:25:52.5	19.565 (0.100)	18.435 (0.164)	
223	00:01:57.33	−15:26:20.8	18.728 (0.052)	17.799 (0.087)	
224	00:01:57.37	−15:26:32.9	18.806 (0.063)	17.827 (0.093)	
225	00:01:57.38	−15:29:22.4	17.740 (0.034)	16.610 (0.031)	
226	00:01:57.39	−15:26:26.4	19.490 (0.111)	19.008 (0.252)	
227	00:01:57.39	−15:27:50.3	19.404 (0.096)	18.578 (0.183)	
228	00:01:57.39	−15:28:27.5	20.057 (0.150)	18.998 (0.243)	
229	00:01:57.40	−15:25:59.6	18.332 (0.043)	17.568 (0.078)	
230	00:01:57.46	−15:26:42.8	19.111 (0.084)	18.371 (0.149)	
231	00:01:57.49	−15:29:06.8	19.522 (0.107)	18.653 (0.191)	
232	00:01:57.51	−15:29:14.4	18.978 (0.066)	18.190 (0.127)	
233	00:01:57.51	−15:29:17.0	16.520 (0.026)	15.648 (0.015)	SC85 16 LC
234	00:01:57.52	−15:26:12.9	18.954 (0.065)	17.902 (0.089)	
235	00:01:57.53	−15:26:11.4	19.405 (0.100)	18.456 (0.149)	
236	00:01:57.54	−15:26:03.1	18.584 (0.060)	17.830 (0.098)	
237	00:01:57.54	−15:27:57.5	18.289 (0.052)	17.611 (0.071)	
238	00:01:57.55	−15:29:02.5	18.510 (0.050)	17.617 (0.078)	
239	00:01:57.58	−15:26:55.1	19.684 (0.120)	18.824 (0.265)	
240	00:01:57.59	−15:26:38.0	19.903 (0.153)	19.150 (0.292)	
241	00:01:57.63	−15:29:11.7	18.472 (0.048)	16.856 (0.040)	BD04
242	00:01:57.66	−15:28:50.1	19.819 (0.119)	18.807 (0.202)	
243	00:01:57.68	−15:26:37.2	20.692 (0.287)	19.438 (0.382)	
244	00:01:57.69	−15:26:42.0	19.680 (0.121)	19.094 (0.288)	
245	00:01:57.70	−15:27:04.9	19.737 (0.127)	18.808 (0.226)	
246	00:01:57.84	−15:28:45.4	18.952 (0.071)	18.182 (0.122)	
247	00:01:57.84	−15:29:02.9	20.302 (0.203)	19.165 (0.331)	
248	00:01:57.85	−15:29:25.0	18.887 (0.050)	17.338 (0.080)	C
249	00:01:57.86	−15:28:17.6	19.876 (0.137)	19.308 (0.406)	
250	00:01:57.86	−15:29:49.2	18.965 (0.057)	18.305 (0.154)	
251	00:01:57.87	−15:25:26.2	20.016 (0.151)	18.844 (0.257)	
252	00:01:57.87	−15:26:49.6	19.086 (0.074)	18.436 (0.148)	
253	00:01:57.88	−15:27:47.3	18.389 (0.051)	17.764 (0.088)	
254	00:01:57.89	−15:28:04.0	17.234 (0.029)	16.392 (0.025)	
255	00:01:57.95	−15:28:34.7	19.169 (0.083)	18.271 (0.147)	
256	00:01:58.00	−15:27:10.5	19.053 (0.060)	18.265 (0.136)	
257	00:01:58.02	−15:28:00.4	18.703 (0.048)	16.922 (0.046)	C
258	00:01:58.04	−15:29:00.6	19.786 (0.118)	18.844 (0.279)	
259	00:01:58.07	−15:27:50.7	19.729 (0.126)	18.748 (0.228)	
260	00:01:58.07	−15:28:04.7	20.744 (0.310)	17.875 (0.096)	C

Table 1. continued.

No	RA	Dec	J	K_S	Note
261	00:01:58.08	−15:27:40.0	13.649 (0.025)	12.915 (0.006)	
262	00:01:58.09	−15:28:02.0	18.058 (0.039)	17.298 (0.053)	
263	00:01:58.10	−15:26:42.2	19.472 (0.089)	18.752 (0.188)	
264	00:01:58.11	−15:26:15.1	19.762 (0.126)	19.064 (0.251)	
265	00:01:58.11	−15:27:03.3	19.129 (0.076)	18.492 (0.185)	
266	00:01:58.12	−15:25:54.5	19.208 (0.183)	17.366 (0.077)	C
267	00:01:58.14	−15:25:37.4	18.594 (0.055)	16.984 (0.046)	C
268	00:01:58.16	−15:25:27.0	19.149 (0.079)	17.839 (0.107)	C
269	00:01:58.16	−15:25:54.7	19.629 (0.256)	17.366 (0.077)	C
270	00:01:58.17	−15:27:47.9	20.312 (0.211)	19.518 (0.424)	
271	00:01:58.19	−15:30:00.2	18.171 (0.035)	16.236 (0.025)	BD04
272	00:01:58.20	−15:29:10.0	19.003 (0.063)	17.737 (0.084)	C
273	00:01:58.24	−15:25:53.5	19.463 (0.122)	18.405 (0.149)	
274	00:01:58.25	−15:25:52.5	18.708 (0.058)	17.740 (0.075)	
275	00:01:58.29	−15:25:40.3	19.201 (0.074)	18.357 (0.157)	
276	00:01:58.29	−15:27:55.3	18.482 (0.049)	17.330 (0.053)	BD04
277	00:01:58.29	−15:28:07.8	19.734 (0.124)	18.420 (0.177)	C
278	00:01:58.36	−15:27:53.9	19.957 (0.160)	18.999 (0.271)	BD04
279	00:01:58.37	−15:25:31.3	20.156 (0.148)	18.954 (0.306)	
280	00:01:58.40	−15:28:00.6	18.762 (0.056)	17.422 (0.061)	BD04
281	00:01:58.41	−15:26:25.5	19.152 (0.062)	18.215 (0.139)	
282	00:01:58.41	−15:29:04.0	19.226 (0.077)	18.101 (0.112)	
283	00:01:58.42	−15:25:36.2	19.505 (0.099)	18.455 (0.190)	
284	00:01:58.44	−15:27:55.1	19.286 (0.091)	18.494 (0.170)	BD04
285	00:01:58.46	−15:26:07.5	18.764 (0.048)	17.653 (0.069)	
286	00:01:58.47	−15:26:09.0	19.612 (0.107)	17.965 (0.097)	C
287	00:01:58.47	−15:26:32.8	19.180 (0.074)	18.041 (0.117)	BD04
288	00:01:58.49	−15:27:20.3	20.011 (0.157)	19.313 (0.364)	
289	00:01:58.50	−15:28:45.0	19.611 (0.099)	18.961 (0.258)	
290	00:01:58.50	−15:29:16.5	19.303 (0.086)	18.236 (0.146)	
291	00:01:58.51	−15:27:29.3	18.507 (0.043)	17.372 (0.059)	
292	00:01:58.54	−15:25:47.9	18.843 (0.054)	17.797 (0.091)	BD04
293	00:01:58.59	−15:28:08.2	18.758 (0.054)	17.748 (0.081)	
294	00:01:58.64	−15:28:03.9	18.483 (0.051)	17.435 (0.062)	
295	00:01:58.65	−15:28:40.5	18.178 (0.043)	17.454 (0.065)	
296	00:01:58.66	−15:26:43.1	20.859 (0.351)	19.636 (0.537)	
297	00:01:58.69	−15:26:15.4	19.303 (0.088)	18.541 (0.170)	
298	00:01:58.69	−15:26:17.7	19.820 (0.137)	18.880 (0.235)	
299	00:01:58.70	−15:28:54.1	19.527 (0.098)	18.608 (0.171)	
300	00:01:58.72	−15:28:02.2	18.645 (0.046)	16.906 (0.055)	C
301	00:01:58.75	−15:26:02.7	18.967 (0.059)	18.022 (0.114)	
302	00:01:58.78	−15:25:35.1	18.873 (0.063)	17.715 (0.090)	
303	00:01:58.83	−15:28:15.9	19.723 (0.111)	16.533 (0.032)	C
304	00:01:58.83	−15:29:32.7	18.599 (0.048)	17.359 (0.063)	BD04
305	00:01:58.85	−15:29:28.5	18.929 (0.056)	17.926 (0.098)	
306	00:01:58.87	−15:27:37.4	18.643 (0.047)	17.283 (0.083)	BD04
307	00:01:58.89	−15:26:39.1	19.080 (0.089)	18.276 (0.171)	
308	00:01:58.89	−15:29:27.5	18.801 (0.057)	17.396 (0.061)	BD04
309	00:01:58.90	−15:30:04.6	18.125 (0.073)	16.393 (0.075)	C
310	00:01:58.94	−15:26:05.6	18.641 (0.052)	17.805 (0.089)	
311	00:01:58.98	−15:25:43.2	18.832 (0.058)	17.938 (0.104)	
312	00:01:59.01	−15:26:31.4	19.080 (0.063)	18.245 (0.129)	
313	00:01:59.02	−15:28:21.4	18.344 (0.037)	16.709 (0.031)	BD04
314	00:01:59.02	−15:28:47.1	19.566 (0.082)	18.824 (0.223)	
315	00:01:59.06	−15:28:32.2	19.542 (0.106)	17.798 (0.092)	C
316	00:01:59.07	−15:27:18.6	18.634 (0.061)	18.169 (0.140)	
317	00:01:59.09	−15:27:00.9	18.177 (0.035)	16.324 (0.024)	BD04
318	00:01:59.09	−15:30:04.0	18.872 (0.061)	17.228 (0.054)	BD04
319	00:01:59.15	−15:28:44.8	19.502 (0.084)	18.688 (0.194)	
320	00:01:59.16	−15:27:15.0	19.608 (0.098)	19.265 (0.366)	
321	00:01:59.16	−15:28:09.5	19.157 (0.084)	18.061 (0.108)	
322	00:01:59.19	−15:29:55.4	19.771 (0.105)	18.260 (0.141)	C
323	00:01:59.20	−15:28:12.9	18.236 (0.051)	16.896 (0.047)	BD04
324	00:01:59.20	−15:28:33.5	18.479 (0.037)	17.749 (0.078)	
325	00:01:59.21	−15:25:52.4	19.840 (0.146)	19.027 (0.266)	
326	00:01:59.23	−15:25:20.5	19.904 (0.147)	18.937 (0.294)	

Table 1. continued.

No	RA	Dec	J	K_S	Note
327	00:01:59.24	−15:29:25.3	19.131 (0.081)	17.754 (0.090)	BD04
328	00:01:59.28	−15:28:30.9	18.885 (0.060)	18.451 (0.152)	
329	00:01:59.30	−15:25:50.2	18.713 (0.052)	17.274 (0.053)	C
330	00:01:59.31	−15:26:07.0	20.066 (0.184)	18.903 (0.239)	
331	00:01:59.35	−15:26:45.8	19.930 (0.117)	19.173 (0.320)	
332	00:01:59.36	−15:27:00.8	18.983 (0.063)	18.332 (0.142)	
333	00:01:59.38	−15:25:22.4	18.769 (0.061)	17.738 (0.116)	
334	00:01:59.38	−15:26:41.4	20.286 (0.204)	19.029 (0.276)	
335	00:01:59.38	−15:27:47.7	18.898 (0.057)	18.015 (0.115)	
336	00:01:59.39	−15:25:36.6	19.313 (0.091)	16.595 (0.032)	C
337	00:01:59.39	−15:26:24.2	19.155 (0.077)	18.381 (0.159)	
338	00:01:59.40	−15:25:47.3	16.527 (0.019)	15.713 (0.015)	
339	00:01:59.40	−15:28:21.6	19.913 (0.144)	19.399 (0.453)	
340	00:01:59.40	−15:29:14.3	18.366 (0.041)	17.593 (0.071)	
341	00:01:59.40	−15:29:44.7	20.381 (0.201)	19.380 (0.392)	
342	00:01:59.43	−15:25:50.7	20.201 (0.215)	19.034 (0.263)	BD04
343	00:01:59.43	−15:27:37.6	18.274 (0.043)	17.256 (0.057)	
344	00:01:59.44	−15:25:44.0	19.215 (0.074)	18.260 (0.138)	
345	00:01:59.44	−15:26:20.7	19.479 (0.094)	18.489 (0.172)	
346	00:01:59.46	−15:29:40.4	19.978 (0.161)	18.913 (0.255)	
347	00:01:59.47	−15:27:04.1	20.234 (0.197)	19.295 (0.363)	
348	00:01:59.48	−15:25:34.2	19.398 (0.104)	18.604 (0.188)	
349	00:01:59.49	−15:27:56.6	17.894 (0.040)	17.129 (0.047)	
350	00:01:59.50	−15:27:34.9	19.069 (0.077)	18.336 (0.142)	
351	00:01:59.50	−15:29:27.4	17.930 (0.029)	17.812 (0.080)	
352	00:01:59.52	−15:27:51.2	19.401 (0.082)	18.965 (0.254)	
353	00:01:59.55	−15:25:50.6	19.829 (0.152)	19.036 (0.247)	
354	00:01:59.56	−15:29:49.0	20.042 (0.447)	16.163 (0.025)	C
355	00:01:59.62	−15:29:50.9	19.316 (0.082)	18.392 (0.140)	
356	00:01:59.64	−15:28:33.8	19.678 (0.102)	18.281 (0.144)	C
357	00:01:59.66	−15:26:48.7	19.817 (0.136)	18.901 (0.238)	
358	00:01:59.68	−15:27:29.5	18.321 (0.032)	17.620 (0.076)	
359	00:01:59.73	−15:25:43.6	19.151 (0.076)	18.483 (0.183)	
360	00:01:59.74	−15:29:42.5	19.007 (0.064)	17.645 (0.081)	BD04
361	00:01:59.83	−15:25:22.2	20.062 (0.159)	19.265 (0.408)	
362	00:01:59.84	−15:26:42.2	20.048 (0.172)	19.440 (0.377)	
363	00:01:59.85	−15:27:18.8	18.696 (0.053)	17.395 (0.061)	BD04
364	00:01:59.85	−15:28:20.0	18.748 (0.052)	18.749 (0.202)	
365	00:01:59.89	−15:28:30.3	19.367 (0.082)	17.712 (0.087)	C
366	00:01:59.90	−15:26:05.3	18.662 (0.054)	17.537 (0.068)	BD04
367	00:01:59.90	−15:29:42.3	18.831 (0.055)	16.724 (0.038)	BD04
368	00:01:59.91	−15:27:59.9	17.951 (0.032)	17.073 (0.048)	
369	00:01:59.93	−15:25:28.8	18.112 (0.028)	16.678 (0.035)	BD04
370	00:01:59.95	−15:27:31.7	18.910 (0.077)	17.871 (0.103)	
371	00:01:59.97	−15:28:32.0	18.407 (0.039)	17.773 (0.087)	
372	00:01:59.98	−15:26:25.4	19.094 (0.073)	18.307 (0.158)	
373	00:01:59.98	−15:29:20.2	19.076 (0.064)	17.672 (0.084)	BD04
374	00:02:00.00	−15:26:19.1	18.086 (0.032)	17.097 (0.048)	
375	00:02:00.00	−15:28:27.1	18.940 (0.065)	18.067 (0.116)	
376	00:02:00.01	−15:26:37.5	18.796 (0.057)	17.489 (0.066)	BD04
377	00:02:00.02	−15:25:31.2	18.373 (0.042)	17.405 (0.066)	
378	00:02:00.03	−15:25:41.1	20.214 (0.166)	18.959 (0.262)	
379	00:02:00.04	−15:28:00.8	19.886 (0.129)	19.024 (0.274)	
380	00:02:00.04	−15:28:53.0	20.074 (0.141)	18.296 (0.145)	C
381	00:02:00.06	−15:27:41.1	19.476 (0.087)	18.564 (0.184)	
382	00:02:00.06	−15:29:53.7	18.959 (0.067)	18.340 (0.142)	
383	00:02:00.07	−15:28:14.3	18.985 (0.065)	18.003 (0.103)	
384	00:02:00.08	−15:28:34.0	18.742 (0.056)	17.885 (0.093)	
385	00:02:00.12	−15:28:02.1	18.649 (0.044)	17.632 (0.076)	
386	00:02:00.13	−15:29:28.8	19.088 (0.071)	18.307 (0.148)	
387	00:02:00.14	−15:29:11.0	19.027 (0.067)	18.049 (0.102)	
388	00:02:00.15	−15:25:26.9	19.962 (0.155)	18.558 (0.195)	C
389	00:02:00.22	−15:28:06.9	19.748 (0.102)	19.011 (0.258)	
390	00:02:00.25	−15:28:23.3	18.811 (0.053)	17.776 (0.092)	
391	00:02:00.26	−15:29:49.3	18.288 (0.058)	16.583 (0.059)	C
392	00:02:00.27	−15:27:02.7	18.818 (0.049)	17.729 (0.091)	

Table 1. continued.

No	RA	Dec	J	K_S	Note
393	00:02:00.27	−15:28:47.0	20.043 (0.137)	19.039 (0.285)	
394	00:02:00.28	−15:25:56.0	20.287 (0.194)	19.484 (0.456)	
395	00:02:00.30	−15:25:35.3	18.786 (0.049)	17.746 (0.086)	
396	00:02:00.31	−15:27:38.5	19.245 (0.085)	18.506 (0.159)	
397	00:02:00.33	−15:26:38.3	19.047 (0.064)	18.487 (0.161)	
398	00:02:00.35	−15:27:03.5	18.544 (0.077)	16.917 (0.070)	C
399	00:02:00.37	−15:28:51.2	19.357 (0.074)	18.503 (0.155)	
400	00:02:00.41	−15:28:20.7	19.606 (0.108)	18.532 (0.175)	
401	00:02:00.42	−15:29:59.2	18.383 (0.045)	17.071 (0.045)	BD04
402	00:02:00.43	−15:28:18.5	19.302 (0.079)	18.350 (0.131)	
403	00:02:00.44	−15:26:48.1	19.448 (0.085)	18.531 (0.177)	
404	00:02:00.44	−15:27:22.9	19.024 (0.063)	18.402 (0.174)	
405	00:02:00.46	−15:28:51.4	19.437 (0.082)	18.519 (0.166)	
406	00:02:00.46	−15:29:00.9	18.606 (0.053)	17.518 (0.073)	
407	00:02:00.52	−15:27:33.6	18.784 (0.054)	17.645 (0.077)	
408	00:02:00.53	−15:28:31.0	18.161 (0.033)	17.937 (0.122)	
409	00:02:00.57	−15:28:02.2	18.765 (0.051)	18.041 (0.104)	
410	00:02:00.57	−15:29:03.9	18.621 (0.054)	18.060 (0.110)	
411	00:02:00.59	−15:29:29.8	18.794 (0.055)	17.453 (0.068)	BD04
412	00:02:00.64	−15:26:59.8	18.997 (0.060)	17.943 (0.091)	
413	00:02:00.65	−15:26:18.2	19.072 (0.085)	18.665 (0.216)	
414	00:02:00.65	−15:27:25.3	18.806 (0.052)	17.323 (0.056)	C
415	00:02:00.71	−15:26:22.7	19.309 (0.086)	18.474 (0.167)	SC85 V28
416	00:02:00.74	−15:25:36.9	20.631 (0.270)	19.371 (0.380)	
417	00:02:00.74	−15:26:30.1	18.391 (0.042)	17.479 (0.065)	
418	00:02:00.75	−15:25:26.9	19.888 (0.151)	18.721 (0.242)	
419	00:02:00.77	−15:27:23.1	20.518 (0.232)	19.695 (0.530)	BD04
420	00:02:00.88	−15:28:16.5	19.029 (0.062)	17.639 (0.074)	C
421	00:02:00.89	−15:28:47.2	19.265 (0.072)	18.236 (0.135)	
422	00:02:00.95	−15:27:47.7	19.555 (0.094)	18.659 (0.192)	
423	00:02:00.99	−15:27:00.3	19.241 (0.076)	18.116 (0.118)	
424	00:02:01.00	−15:28:02.8	20.116 (0.166)	19.009 (0.262)	
425	00:02:01.00	−15:28:36.1	16.843 (0.025)	15.953 (0.019)	SC85 V32 LC
426	00:02:01.02	−15:25:27.8	20.293 (0.201)	19.319 (0.406)	
427	00:02:01.02	−15:25:44.8	18.601 (0.043)	17.327 (0.064)	C
428	00:02:01.06	−15:25:32.0	20.172 (0.197)	19.210 (0.357)	
429	00:02:01.06	−15:29:56.9	18.566 (0.049)	16.930 (0.045)	BD04
430	00:02:01.07	−15:26:22.8	19.265 (0.077)	18.360 (0.153)	
431	00:02:01.09	−15:27:23.1	20.208 (0.162)	19.123 (0.292)	
432	00:02:01.11	−15:25:43.1	19.745 (0.118)	18.637 (0.204)	BD04
433	00:02:01.14	−15:30:07.8	19.494 (0.091)	18.668 (0.220)	
434	00:02:01.16	−15:27:42.3	19.179 (0.075)	18.270 (0.130)	
435	00:02:01.17	−15:25:31.3	19.795 (0.132)	18.689 (0.218)	
436	00:02:01.20	−15:29:13.8	20.154 (0.151)	18.977 (0.262)	
437	00:02:01.22	−15:27:15.3	18.271 (0.041)	16.845 (0.036)	BD04
438	00:02:01.26	−15:25:38.8	19.218 (0.066)	17.304 (0.061)	BD04
439	00:02:01.29	−15:27:29.2	19.117 (0.079)	18.028 (0.102)	
440	00:02:01.31	−15:29:17.2	19.505 (0.084)	16.721 (0.040)	C
441	00:02:01.32	−15:26:15.0	19.345 (0.083)	18.193 (0.125)	
442	00:02:01.32	−15:27:41.8	18.479 (0.043)	17.509 (0.071)	
443	00:02:01.33	−15:27:00.2	19.356 (0.089)	18.181 (0.123)	
444	00:02:01.33	−15:28:38.2	17.521 (0.029)	16.078 (0.022)	C
445	00:02:01.34	−15:27:31.1	17.171 (0.026)	16.777 (0.036)	
446	00:02:01.34	−15:29:20.6	19.205 (0.083)	17.679 (0.090)	BD04
447	00:02:01.38	−15:28:47.3	20.023 (0.147)	18.618 (0.196)	C
448	00:02:01.40	−15:27:28.9	18.544 (0.048)	16.866 (0.038)	BD04
449	00:02:01.41	−15:26:47.4	18.530 (0.045)	17.855 (0.099)	
450	00:02:01.43	−15:27:50.2	19.919 (0.154)	19.306 (0.360)	
451	00:02:01.45	−15:25:19.7	20.056 (0.216)	19.147 (0.456)	
452	00:02:01.45	−15:28:28.1	19.186 (0.079)	18.224 (0.130)	

Table 1. continued.

No	RA	Dec	J	K_S	Note
453	00:02:01.48	−15:26:05.3	19.326 (0.087)	18.242 (0.122)	
454	00:02:01.50	−15:27:14.2	20.488 (0.231)	17.020 (0.043)	C
455	00:02:01.50	−15:28:38.1	19.008 (0.057)	18.031 (0.103)	BD04
456	00:02:01.54	−15:26:52.5	17.891 (0.086)	16.455 (0.052)	C
457	00:02:01.58	−15:26:52.4	18.704 (0.168)	16.455 (0.052)	C
458	00:02:01.62	−15:29:27.5	19.539 (0.088)	17.988 (0.108)	BD04
459	00:02:01.66	−15:25:49.9	19.032 (0.058)	18.187 (0.126)	
460	00:02:01.73	−15:26:11.3	16.879 (0.024)	15.839 (0.016)	
461	00:02:01.74	−15:28:45.7	18.914 (0.062)	17.511 (0.069)	C
462	00:02:01.76	−15:29:07.9	19.467 (0.099)	18.282 (0.140)	
463	00:02:01.81	−15:28:52.5	20.263 (0.174)	19.095 (0.301)	
464	00:02:01.82	−15:29:36.7	18.932 (0.056)	17.630 (0.082)	C
465	00:02:01.89	−15:25:49.9	19.988 (0.154)	18.885 (0.259)	
466	00:02:01.89	−15:26:23.0	16.106 (0.020)	15.371 (0.012)	
467	00:02:01.94	−15:27:47.9	18.434 (0.045)	17.035 (0.049)	BD04
468	00:02:01.96	−15:27:02.7	19.869 (0.140)	17.260 (0.057)	C
469	00:02:01.99	−15:28:30.1	19.267 (0.082)	17.809 (0.096)	BD04
470	00:02:02.01	−15:25:25.3	19.233 (0.078)	18.033 (0.128)	
471	00:02:02.04	−15:26:04.1	19.317 (0.081)	18.211 (0.124)	
472	00:02:02.04	−15:29:03.0	19.934 (0.131)	18.651 (0.190)	C
473	00:02:02.05	−15:26:17.0	19.917 (0.147)	18.903 (0.264)	
474	00:02:02.05	−15:26:20.5	19.256 (0.107)	18.208 (0.138)	
475	00:02:02.05	−15:26:22.3	18.699 (0.055)	16.831 (0.033)	C
476	00:02:02.10	−15:27:33.7	20.190 (0.167)	19.118 (0.327)	
477	00:02:02.11	−15:28:51.2	20.014 (0.140)	18.952 (0.280)	
478	00:02:02.12	−15:26:55.4	19.930 (0.155)	18.814 (0.223)	
479	00:02:02.16	−15:26:19.9	17.767 (0.031)	16.644 (0.034)	BD04
480	00:02:02.17	−15:28:33.7	19.433 (0.140)	18.237 (0.152)	
481	00:02:02.17	−15:29:37.1	19.356 (0.075)	18.343 (0.137)	
482	00:02:02.20	−15:27:44.3	18.639 (0.052)	17.291 (0.058)	C
483	00:02:02.23	−15:27:35.7	19.561 (0.103)	18.520 (0.176)	
484	00:02:02.25	−15:26:01.4	18.924 (0.059)	17.942 (0.096)	
485	00:02:02.25	−15:27:29.3	19.720 (0.110)	19.334 (0.378)	
486	00:02:02.27	−15:26:53.7	19.850 (0.127)	18.975 (0.261)	
487	00:02:02.33	−15:25:51.0	19.062 (0.071)	17.315 (0.056)	BD04
488	00:02:02.35	−15:26:24.6	19.473 (0.094)	18.742 (0.223)	
489	00:02:02.38	−15:26:10.8	19.493 (0.096)	17.946 (0.115)	BD04
490	00:02:02.39	−15:26:33.3	19.782 (0.117)	19.081 (0.288)	
491	00:02:02.40	−15:28:12.2	18.817 (0.063)	17.086 (0.051)	BD04
492	00:02:02.43	−15:27:16.8	19.745 (0.139)	18.814 (0.228)	
493	00:02:02.52	−15:27:32.1	20.331 (0.192)	19.514 (0.481)	
494	00:02:02.60	−15:28:21.8	20.160 (0.167)	18.931 (0.245)	
495	00:02:02.60	−15:29:49.3	20.138 (0.159)	19.184 (0.305)	
496	00:02:02.61	−15:27:49.8	19.735 (0.109)	18.827 (0.248)	
497	00:02:02.67	−15:26:03.3	19.213 (0.077)	18.165 (0.132)	
498	00:02:02.68	−15:26:24.1	20.889 (0.372)	19.108 (0.288)	
499	00:02:02.68	−15:29:14.8	19.019 (0.058)	17.928 (0.103)	
500	00:02:02.69	−15:29:01.2	18.989 (0.056)	17.001 (0.048)	C
501	00:02:02.71	−15:28:14.5	20.125 (0.146)	19.279 (0.356)	
502	00:02:02.74	−15:27:16.8	18.478 (0.062)	16.787 (0.067)	C
503	00:02:02.77	−15:27:55.0	19.327 (0.072)	16.825 (0.040)	C
504	00:02:02.83	−15:29:58.7	18.806 (0.052)	17.046 (0.056)	C
505	00:02:02.84	−15:26:38.2	19.401 (0.082)	18.424 (0.171)	
506	00:02:03.04	−15:28:24.1	18.743 (0.051)	16.997 (0.041)	C
507	00:02:03.07	−15:28:17.0	18.662 (0.042)	18.239 (0.143)	
508	00:02:03.09	−15:26:17.5	18.813 (0.056)	17.249 (0.056)	C
509	00:02:03.10	−15:28:10.9	19.643 (0.116)	18.693 (0.195)	
510	00:02:03.14	−15:27:56.0	19.806 (0.134)	19.117 (0.339)	
511	00:02:03.18	−15:25:39.1	17.786 (0.026)	16.621 (0.033)	
512	00:02:03.28	−15:28:57.5	20.162 (0.155)	19.096 (0.296)	
513	00:02:03.34	−15:25:47.6	19.513 (0.107)	18.286 (0.150)	C
514	00:02:03.43	−15:26:22.8	17.998 (0.032)	17.161 (0.052)	SC85 V27
515	00:02:03.46	−15:29:50.0	19.966 (0.144)	18.290 (0.141)	C
516	00:02:03.49	−15:25:48.2	20.347 (0.187)	19.165 (0.326)	

Table 1. continued.

No	RA	Dec	J	K_S	Note
517	00:02:03.50	−15:26:10.1	20.057 (0.182)	18.957 (0.283)	
518	00:02:03.56	−15:27:23.9	18.755 (0.059)	17.132 (0.068)	C
519	00:02:03.58	−15:26:18.0	19.208 (0.079)	18.096 (0.132)	
520	00:02:03.61	−15:27:13.6	20.087 (0.181)	19.413 (0.473)	
521	00:02:03.62	−15:26:10.9	20.674 (0.294)	19.478 (0.458)	
522	00:02:03.62	−15:27:06.0	20.180 (0.190)	19.002 (0.299)	
523	00:02:03.64	−15:29:57.5	20.524 (0.255)	19.022 (0.325)	
524	00:02:03.65	−15:27:02.1	19.242 (0.087)	18.216 (0.175)	
525	00:02:03.66	−15:27:00.0	18.157 (0.046)	17.179 (0.059)	
526	00:02:03.71	−15:25:48.1	19.933 (0.165)	18.688 (0.238)	C
527	00:02:03.73	−15:25:38.4	19.984 (0.134)	19.031 (0.366)	
528	00:02:03.73	−15:27:07.6	19.076 (0.071)	17.405 (0.074)	C
529	00:02:03.75	−15:27:33.6	19.332 (0.092)	18.308 (0.170)	
530	00:02:03.76	−15:25:43.5	18.961 (0.068)	17.706 (0.116)	C
531	00:02:03.77	−15:26:08.7	20.206 (0.200)	19.226 (0.431)	
532	00:02:03.78	−15:28:47.6	19.561 (0.124)	17.857 (0.129)	C
533	00:02:03.80	−15:26:25.8	20.254 (0.198)	19.299 (0.438)	
534	00:02:03.83	−15:26:17.2	20.352 (0.229)	19.286 (0.512)	
535	00:02:03.84	−15:27:48.9	20.154 (0.190)	17.218 (0.069)	C
536	00:02:03.85	−15:25:39.2	20.323 (0.244)	19.453 (0.514)	
537	00:02:03.85	−15:28:13.7	20.634 (0.306)	19.454 (0.528)	
538	00:02:03.90	−15:25:47.9	15.330 (0.042)	14.538 (0.014)	
539	00:02:03.92	−15:29:30.3	19.927 (0.136)	19.397 (0.488)	
540	00:02:03.95	−15:25:40.6	20.528 (0.293)	18.853 (0.299)	
541	00:02:03.98	−15:26:30.2	19.160 (0.072)	17.724 (0.094)	C
542	00:02:04.03	−15:28:02.4	19.726 (0.145)	18.585 (0.238)	
543	00:02:04.07	−15:27:57.6	19.509 (0.102)	19.254 (0.413)	
544	00:02:04.10	−15:29:42.3	19.175 (0.086)	18.862 (0.315)	
545	00:02:04.14	−15:28:19.4	20.080 (0.199)	19.128 (0.369)	
546	00:02:04.17	−15:28:43.9	21.066 (0.421)	19.635 (0.516)	
547	00:02:04.24	−15:28:07.5	19.461 (0.108)	17.947 (0.136)	C
548	00:02:04.31	−15:29:17.9	20.089 (0.182)	18.977 (0.338)	
549	00:02:04.33	−15:29:11.2	19.269 (0.079)	17.796 (0.118)	C
550	00:02:04.42	−15:25:42.0	20.075 (0.177)	18.779 (0.355)	
551	00:02:04.46	−15:26:14.1	20.598 (0.299)	18.971 (0.375)	
552	00:02:04.47	−15:27:16.0	19.690 (0.129)	17.135 (0.088)	C
553	00:02:04.52	−15:27:44.5	19.947 (0.159)	19.182 (0.486)	
554	00:02:04.52	−15:29:37.6	18.040 (0.046)	16.760 (0.126)	C
555	00:02:04.60	−15:27:07.5	20.153 (0.194)	19.296 (0.533)	